Solar Energy
And Sustainable Development
Refereed, biannual scientific journal issued by:
The Libyan Center for Solar Energy Research and Studies

# Study of Aluminium, Gallium and Gallium Boron as P-Type Dopants for New-Generation n+np+ Solar Cells

**H. Korichi[1]*, A. Boucheham[2], M. Kezrane[1].**

[1]Yahia Fares University, Department of mechanical engineering, LMP2M, Medea, Algeria.
[2]Research Center in Semiconductor Technology for Energetics, DDCS Division, Algeria.

E-*mail:* korichi.hakim@univ-medea.dz , aghaniboucheham@gmail.com , mohamed.kezrane@yahoo.fr .

## ARTICLE INFO.

Article history:
Received 12 May 2024
Received in revised form 13 May 2024
Accepted 4 Oct 2024
Available online 9 Oct 2024

## KEYWORDS

n+np+ silicon solar cells, gallium doping, boron doping, co-doping, surface passivation.

## ABSTRACT

Silicon n-type n+np+ solar cells offer many advantages over conventional n+pp+ cells, including better resistance to light-induced degradation and higher conversion efficiency potential. However, the formation of the p+ emitter in n+np+ cells requires high diffusion temperatures and the use of alternative boron dopants is necessary to overcome the limitations of conventional processes. This study explored aluminium, gallium and gallium/boron co-doping as p-type dopants for the fabrication of thin (140 µm) n+np+ solar cells.

The results showed that aluminium is not suitable for the formation of the p+ emitter due to its low solid solubility in silicon and its high segregation towards silicon oxide. Gallium required high diffusion temperatures and suffered from a degradation of the concentration profile in later stages of the manufacturing process, leading to poor performing solar cells. Gallium/boron co-doping has proved to be a promising alternative to boron. Thin n+np+ solar cells doped with GaB achieved a maximum conversion efficiency of 13.7%, slightly lower than that of boron-doped cells (14.9%). Optimisation of the GaB diffusion process and surface passivation could further improve the performance of these cells. This study demonstrates the potential of gallium/boron co-doping for the manufacture of new-generation thin n+np+ solar cells. Further research is needed to fully exploit the advantages of this technology and contribute to improving the efficiency and cost of silicon solar cells.

*Corresponding author.

DOI: https://doi.org/10.51646/jsesd.v13i2.195

# دراسة الألومنيوم والغاليوم وغاليوم البورون كمواد منشّطة من النوع P للجيل الجديد من الخلايا الشمسية n+np+

قريشي حكيم ، بوشحم عبد الغاني، قزران محمد.

**ملخص**: توفر الخلايا الشمسية السيليكونية من النوع n+np+ العديد من المزايا مقارنةً بخلايا n+pp+ التقليدية، بما في ذلك مقاومة أفضل للتدهور الناتج عن الضوء وإمكانية تحويل أعلى كفاءة. ومع ذلك، فإن تكوين الباعث p+ في خلايا n+np+ يتطلب درجات حرارة انتشار عالية، كما أن استخدام منشطات البورون البديلة ضروري للتغلب على قيود العمليات التقليدية. استكشفت هذه الدراسة منشطات الألومنيوم والغاليوم والغاليوم/البورون المشتركة كمواد منشّطة من النوع p لتصنيع خلايا شمسية رقيقة (140 ميكرومتر) من النوعn+np +. أظهرت النتائج أن الألومنيوم غير مناسب لتكوين الباعثp + بسبب انخفاض قابليته للذوبان الصلب في السيليكون وانفصاله العالي تجاه أكسيد السيليكون. وتطلب الغاليوم درجات حرارة انتشار عالية وعانى من تدهور في شكل التركيز في مراحل لاحقة من عملية التصنيع، مما أدى إلى ضعف أداء الخلايا الشمسية. وقد أثبت الغاليوم/البورون المشترك أنه بديل واعد للبورون. حققت الخلايا الشمسية الرقيقة n+np+ المخدرة بـ GaB كفاءة تحويل قصوى بلغت 13.7%، وهي أقل قليلاً من الخلايا المخدرة بالبورون (14.9%). يمكن أن يؤدي تحسين عملية نشر الغاليوم الغاليبي والتخميل السطحي إلى تحسين أداء هذه الخلايا. توضح هذه الدراسة إمكانية استخدام المنشطات المشتركة بين الغاليوم/البورون لتصنيع الجيل الجديد من الخلايا الشمسية الرقيقة n+np+. هناك حاجة إلى إجراء المزيد من الأبحاث للاستفادة الكاملة من مزايا هذه التقنية والمساهمة في تحسين كفاءة وتكلفة الخلايا الشمسية السيليكونية.

**الكلمات المفتاحية** – خلايا السليكون الشمسية n+np+، منشطات الغاليوم، منشطات البورون، المنشطات المشتركة، تخميل السطح.

## 1. INTRODUCTION

The photovoltaic sector is experiencing unprecedented growth, driven by the need to combat climate change and ensure a sustainable energy future. By 2023, global installed solar PV capacity is expected to reach 1,177 GW, reflecting a global transition to renewable and sustainable energy technologies [1]. This trend is also reflected in Libya, where the aim is to increase the share of renewable energy to 25% by 2025 and to more than 50% by 2050, focusing mainly on solar energy (mainly photovoltaic and thermal) and wind power [2]. In this context, crystalline silicon solar cells largely dominate the photovoltaic market [3, 4]. The majority of them are manufactured on boron-doped p-type substrates with a conventional n+pp+ structure [5]. However, there is growing interest in the use of phosphorus-doped n-type substrates due to their intrinsic advantages, including longer minority carrier lifetimes and reduced sensitivity to transition metal contamination [6]. These characteristics give n+np+ cells a higher efficiency potential, justifying current research efforts aimed at optimising p+ doping techniques [7].

The formation of an efficient p+ emitter in n+np+ cells presents specific challenges. Boron diffusion, although established for n+pp+ cells, requires high temperatures that can damage thin substrates and generate a boron-rich layer (BRL) that is detrimental to performance [8], [9]. Aluminium, a common p+ dopant in the semiconductor industry, is limited in photovoltaics due to its low solubility in silicon and high segregation to silicon oxide, making it difficult to form high-quality p+ emitters [10]. In addition, n+np+ cells offer increased resistance to light-induced degradation (LID) associated with boron-oxygen interaction, a phenomenon affecting p-type cells that can lead to a decrease in open-circuit voltage (Voc) [11], [12].To overcome these limitations, the exploration of alternative dopants, such as gallium and gallium/boron co-doping, is proving promising. Gallium has a higher diffusion coefficient than boron, which reduces diffusion temperatures and thermal damage [13], a particularly important aspect for thin solar cells sensitive to degradation induced by high-temperature treatments [14]. Gallium/boron co-doping combines the advantages of each element, improving the quality of the p+ emitter [15]. Recent studies have demonstrated the potential of this approach for the fabrication of high-efficiency n+np+ solar cells [16].

In this study, we evaluate aluminium, gallium and gallium/boron co-doping as p-type dopants for the fabrication of new generation n+np+ solar cells on 140 μm thick n-type silicon substrates. We investigated the influence of diffusion parameters (temperature, time, gas) on the resistance per square (R□) and the impurity concentration profile in the p+ region. Solar cells were fabricated and characterised in order to compare their electrical and optical performance. These analyses will make it possible to identify the most appropriate p+ dopant for the creation of low-cost, highly efficient n+np+ cells, while taking into account the limitations associated with the use of thin substrates, and will thus contribute to the advancement of photovoltaic technologies, in line with current research efforts in the field [17].

## 2. Materials And Methods

### 2.1. Substrates and Sample Preparation

Solar-grade, phosphorus-doped, n-type single-crystal silicon substrates with {100} orientation were used in this study. The substrates were initially 240 μm thick and 100 mm in diameter. A thinning process using a KOH solution was carried out to obtain substrates with a final thickness of 140 μm ± 10 μm, following the methodology described by Prem Pa et al.
The surface of the substrates was textured using an anisotropic etching process based on KOH, isopropyl alcohol and deionised water. This step creates micro-pyramids on the silicon surface, reducing the reflection of incident light and improving light absorption in the solar cell [18].
Diffusion of p+ dopants
Various p+ dopants were studied for the formation of the emitter: boron (PBF20), aluminium (Al110), gallium (Ga252), gallium/boron (GaB260) and aluminium/gallium (AlGa130), all supplied by Filmtronics. The dopants were deposited by spin-coating using a spinner The spin-coating parameters were adjusted for each dopant to obtain a homogeneous film thickness.
The doped substrates were then subjected to diffusion heat treatment in a quartz tube furnace. The diffusion temperature and duration were varied for each dopant in order to optimise the sheet resistance of the p+ region and obtain values between 40 and 60 Ω/□. Different diffusion atmospheres were also tested, including nitrogen (N2), oxygen (O2) and argon (Ar). Recent studies have explored the impact of the scattering atmosphere on the properties of gallium-doped p+ emitters, showing the importance of optimising this parameter [19].

### 2.2. Characterisation of P+ Regions

The Sheet Resistance (R□) Of The p+ regions were measured using the four-tip technique. This technique allows the resistivity of the doped layer to be determined and the uniformity of diffusion over the substrate surface to be assessed.
A CVP21 profiler was used to use the electrochemical capacitance-voltage (ECV) approach to determine the impurity percentage profile as a function of depth. This technique allows the dopant concentration to be measured at different depths in the substrate and the depth of the p-n junction to be determined. ECV analysis is widely used to characterise p+ emitters in solar cells and provides valuable information on dopant distribution and junction formation.

### 2.3. Manufacturing Solar Cells

**The n+np+ solar cells were fabricated using a standard process consisting of the following steps:**
Diffusion of the n+ (phosphorus) dopant: After formation of the p+ emitter, the opposite side of the substrate was doped with phosphorus using POCl3 as the dopant source and a diffusion process at 845°C [20].

**Surface passivation:** A SiO2 film was deposited on both sides of the cell by thermal growth at 800°C To minimize the surface recombination of charge carriers . Surface passivation is essential to improve solar cell performance, particularly for thin cells where surface recombination can be significant [21].

**Deposition of the anti-reflection film:** A 25 nm TiO2 film was deposited by vacuum evaporation on the front face of the cell to minimise reflection of incident light [9]. The choice of material and thickness of the anti-reflection film is crucial to optimise light absorption in the solar cell [22].

**Metallization:** Electrical contacts were screen-printed using silver (Ag) pastes on the front and aluminium/silver (Al/Ag) pastes on the back. The firing temperature of the pastes was optimised for each type of cell. Screen printing metallisation is a common technique for large-scale solar cell production, but requires careful optimisation to minimise resistive losses and recombination at contacts [23].

**Edge insulation:** The edges of the cells were laser-cut to avoid short circuits.

### 2.4. Characterisation of the Solar Cells

The solar cells were characterised by measuring their electrical parameters (short-circuit current (Jsc), open-circuit voltage (Voc), Fill Factor (FF) and conversion efficiency (η)) under standard illumination (AM1.5G, 1000 W/m²), using a Newport Oriel Sol3A Class AAA solar simulator. The cell temperature was maintained at 25°C during the measurements using a temperature control system integrated into the simulator. The spectral response and internal quantum efficiency were also measured to analyse the optical performance of the cells. The characterisation of solar cells makes it possible to assess their conversion efficiency and identify the factors limiting their performance.

## 3. Results And Discussion

### 3.1. Influence of Diffusion Parameters On P+ Regions

The diffusion results for the different p+ dopants are summarised in (Table 1) The objective was to obtain p+ regions with a sheet resistance (R□) between 35 and 60 Ω/□, an ideal value for the formation of screen-printed metallized n+np+ solar cells.

Table 1. Diffusion processes for the B, Ga, GaB, Al and AlGa dopants and the resistance per square of the p+ regions were carried out at different temperatures, times and gases.

| Proc. | Elem. | Gases | Post-diffusion oxidation | post-diffusionTime (min.) | T (°C) | Sheet resistance (Ω/□) |
|---|---|---|---|---|---|---|
| 10 | B | N2 / O2 | Yes | 20 | 970 | 53,0 ± 1,9 |
| 17 | | Ar / O2 | Yes | 20 | 970 | 55 ± 3 |
| 12 | | N2 | Yes | 20 | 1050 | 470 ± 30 |
| 14 | | N2 | NO | 60 | 1050 | 296 ± 111 |
| 18 | | Ar | Yes | 60 | 1100 | 171 ± 9 |
| 20 | | N2 | Yes | 120 | 1100 | 1870 ± 31 |
| 11 | | N2 | Yes | 20 | 1020 | 37,2 ± 2,8 |
| 12 | GaB | N2 | YES | 20 | 970 | 90 ± 7 |
| 17 | | Ar / O2 | Yes | 20 | 970 | 82 ± 8 |
| 26 | | N2 / O2 | Yes | 20 | 970 | 52,9 ± 1,0 |
| 26 | | N2 / O2 | Yes | 20 | 1020 | 36 ± 3 |

| | | | | | | |
|---|---|---|---|---|---|---|
| 10 | | N2 | Yes | 20 | 970 | 55 ± 5 |
| 14 | Al | N2 | NO | 60 | 1050 | 660 ± 20 |
| 18 | | Ar | Yes | 60 | 1100 | 520 ± 190 |
| 12 | | N2 | Yes | 30 | 1050 | 200 ± 50 |
| 13 | | N2 | Yes | 60 | 1050 | 560 ± 30 |
| 14 | AlGa | N2 | NO | 60 | 1050 | 660 ± 20 |
| 18 | | Ar | Yes | 60 | 1100 | 255 ± 26 |
| 20 | | N2 | Yes | 120 | 1100 | 255 ± 28 |

**Boro (B):** Boro, the reference dopant, was able to obtain p+ regions with an R□ of 53-55 Ω/□ for diffusion at 970 °C for 20 min, confirming the results obtained in previous studies.

**Gallium (Ga):** Gallium required higher diffusion temperatures and longer times than boron to obtain compatible R□ values. An R□ of 171 Ω/□ was achieved for diffusion at 1100 °C for 60 minutes. Gallium concentration profiles (Figure 4.1) show greater junction depths than boron, which may be advantageous for some applications.

**Aluminium (Al):** Aluminium did not yield p+ regions with sufficiently low R□, even for scatterings at 1100 °C for 120 min. The low solid solubility of aluminium in silicon and its strong segregation towards silicon oxide explain these results.

**Gallium/boron (GaB):** GaB co-doping has proved to be a promising alternative to boron. P+ regions with an R□ of 37 Ω/□ were obtained for diffusion at 1020 °C for 20 min. The concentration profiles of GaB (Figure 1) show similar characteristics to boron, with a slightly higher surface concentration.

**Aluminium/gallium (AlGa):** AlGa required high diffusion temperatures (1100°C) to achieve an acceptable R□ (255 Ω/□). The complexity of the process and the high cost of AlGa limit its interest for solar cell production.

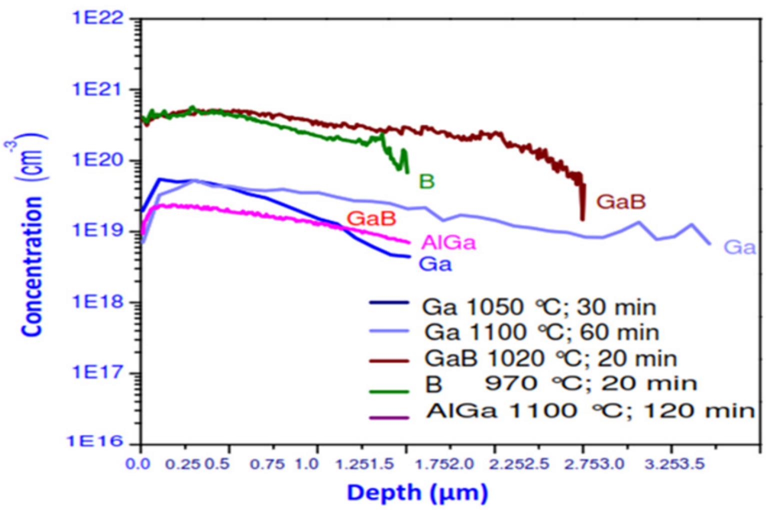


Figure 1. Impurity concentration profiles as a function of depth with Ga, GaB, AlGa and B dopants for different diffusion times and temperatures.

### 3.2. Influence of paste firing temperature

The firing temperature of the metallisation pastes was optimised for boron-doped n+np+ solar cells. The results are presented in (Tables 2 and 3) the best conversion efficiency (14.9%) was obtained for a firing temperature of 840°C and 850°C. Above 860°C, Cell performance begins to

decline due to degradation of the p-n junction and increased contact resistance.
Table 2. Average electrical characteristics of 120 μm thick solar cells as a function of paste firing temperature.

Table 2. Average electrical characteristics of 120 μm thick solar cells as a function of paste firing temperature.

| Dopant p+ | T firing (°C) | cells N° | Voc (mV) | Jsc (mA/cm²) | FF | η (%) |
|---|---|---|---|---|---|---|
| Boron | 840 | 02 | 589,9 ± 1,2 | 33,5 ± 0,8 | 0,740 ± 0,001 | 14,8 ± 0,4 |
| | 850 | 04 | 588,6 ± 2,2 | 33,6 ± 0,4 | 0,739 ± 0,011 | 14,7 ± 0,3 |
| | 860 | 10 | 586,5 ± 2,0 | 33,7 ± 0,3 | 0,738 ± 0,009 | 14,7 ± 0,4 |
| | 870 | 05 | 583,2 ± 2,2 | 34,2 ± 0,3 | 0,719 ± 0,007 | 14,4 ± 0,4 |
| | 880 | 05 | 578,0 ± 3,7 | 34,1 ± 0,1 | 0,695 ± 0,015 | 13,8 ± 0,4 |
| | 890 | 05 | 574,8 ± 5,9 | 33,8 ± 0,9 | 0,697 ± 0,009 | 13,6 ± 0,6 |

Table 3. Electrical characteristics of the best-performing solar cells as a function of paste baking temperature.

| Dopant p+ | T firing (°C) | Voc (mV) | Jsc (mA/cm²) | FF | η (%) |
|---|---|---|---|---|---|
| Boron | 840 | 588,0 | 33,9 | 0,738 | 14,9 |
| | 850 | 590,9 | 33,2 | 0,751 | 14,9 |
| | 860 | 589,8 | 33,9 | 0,739 | 14,8 |
| | 870 | 586,1 | 34,4 | 0,724 | 14,6 |
| | 880 | 582,5 | 34,1 | 0.711 | 14.1 |
| | 890 | 581,6 | 34,5 | 0,707 | 14.2 |

## 3.3. Comparison of solar cell performance

The performance of n+np+ solar cells fabricated with different p+ dopants is compared in (Tables 4,5 and 6) Boro (B): Boron-doped cells achieved a maximum efficiency of 14.9%, confirming the excellent performance of use this dopant to create thin n+np+ solar cells.

Table 4. Average electrical characteristics of n+np+ solar cells doped with aluminium or boron.

| Dopant p+ | T firing (°C) | TD (min) | cells N° | Voc (mV) | Jsc (mA/cm²) | FF | η (%) |
|---|---|---|---|---|---|---|---|
| Boron | 970 | 20 | 06 | 584,4 ± 1,4 | 33,6 ± 0.3 | 0.739±0.007 | 14.6± 0.2 |
| AL | 970 | 20 | 06 | 58 ± 31 | 2,9 ± 0.5 | 0.245 0.005 | 0.04±0.03 |

Table 4 highlights the significant difference in performance between boron-doped and aluminium-doped cells. Boron-doped cells show electrical characteristics typical of functional solar cells, while aluminium-doped cells show signs of short-circuiting, indicating the inefficiency of aluminium as a p+ dopant in this case.

Table 5. Average electrical parameters of n+np+ solar cells fabricated with GaB and B. The diffusion time was maintained at 20 minutes for all processes.

| Dopant p+ | T firing (°C) | T diffusion (min) | cells N° | Voc (mV) | Jsc (mA/cm²) | FF | η (%) |
|---|---|---|---|---|---|---|---|
| Ga | 1050 | 30 | 03 | 106 ± 57 | 2,2 ± 0.4 | 0.253± 0.008 | 0,06 ± 0,05 |
| | 1050 | 60 | 01 | 44 | 2.1 | 0.25 | 0.02 |
| | 1100 | 60 | 04 | 28.7 ± 1.5 | 2,2 ± 0.1 | 0.246± 0.002 | 0.015±0.001 |
| | 1020 | 20 | 04 | 224 ± 61 | 2,5 ± 1.1 | 0.31± 0.06 | 0.15± 0.04 |

Table 5 shows that gallium, despite increasing temperature and diffusion time, failed to produce very efficient solar cells. The low values of Voc, Jsc, FF and η indicate an inefficient p-n junction.

Table 6. Comparison of optimal electrical parameters of n+np+ solar cells doped with Boron and GaB.

| Parameter | Bore | GaB |
|---|---|---|
| Voc (mV) | 590.9 | 588.8 |
| Jsc (mA/cm²) | 33.2 | 33.5 |
| FF | 0.751 | 0.739 |
| η (%) | 14.9 | 13.7 |

- **Boron (B):** Boron-doped cells achieved a maximum efficiency of 14.9%, confirming the excellent performance of this dopant for the creation of thin n+np+ solar cells.
- **Gallium (Ga):** Gallium-doped cells showed very poor electrical performance, with a peak efficiency of just 0.2%. The degradation of the gallium concentration profile during the phosphorus diffusion and oxidation stages could explain these results.
- **Gallium/boron (GaB):** GaB enabled solar cells to be obtained with a maximum efficiency of 13.7%, a value slightly lower than that of boron-doped cells. The presence of a parallel resistor, observed on the J-V curves (Figure 2), contributed to the reduction in Fill Factor and efficiency. Analysis of the J-V curves for GaB-doped cells revealed the presence of a parallel resistance of approximately 150 Ω-cm². This additional resistance contributes to a decrease in the Fill Factor and partly explains the slightly lower efficiency (13.7%) compared with Boron-doped cells.
- **Aluminium (Al):** Aluminium failed to produce functional solar cells, confirming its unsuitability for the formation of the p+ emitter.

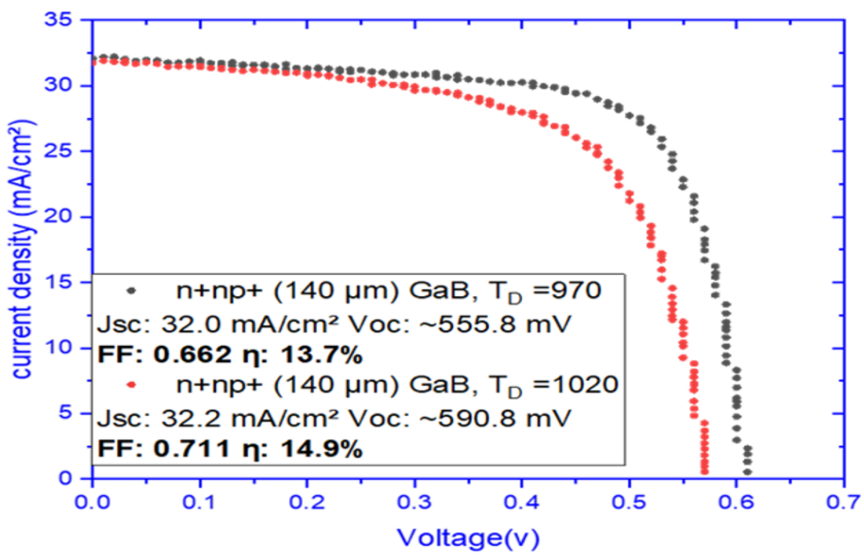


Figure 2. J-V curves for the most efficient gallium-boron doped solar cells. Diffusion lasted 20 minutes.

### 3.4. Analysis of Spectral Response and Internal Quantum Efficiency

The spectral response and internal quantum efficiency (IQE) of boron-doped and GaB-doped solar cells were measured and compared (Figures 3, 4 and 5). The results show a better collection of charge carriers for the boron-doped cells, which explains their higher efficiency.

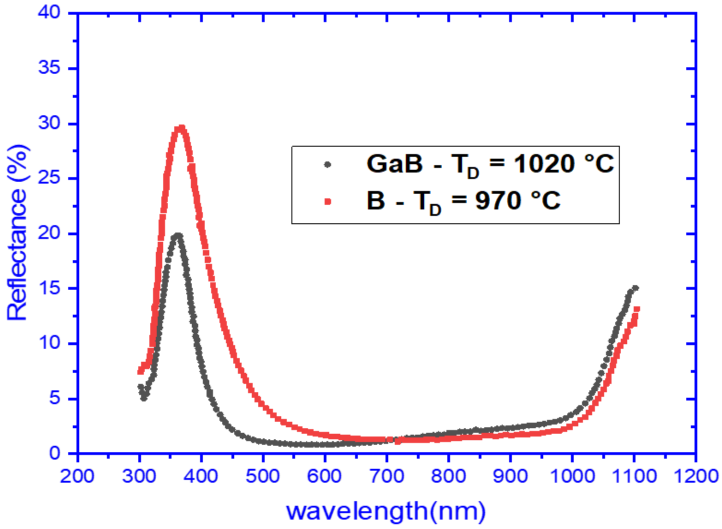


Figure 3. Spectral reflectance of the best-performing solar cells treated with B and GaB. The surface of the devices was coated with thermally deposited SiO2 and TiO2 (25 nm).

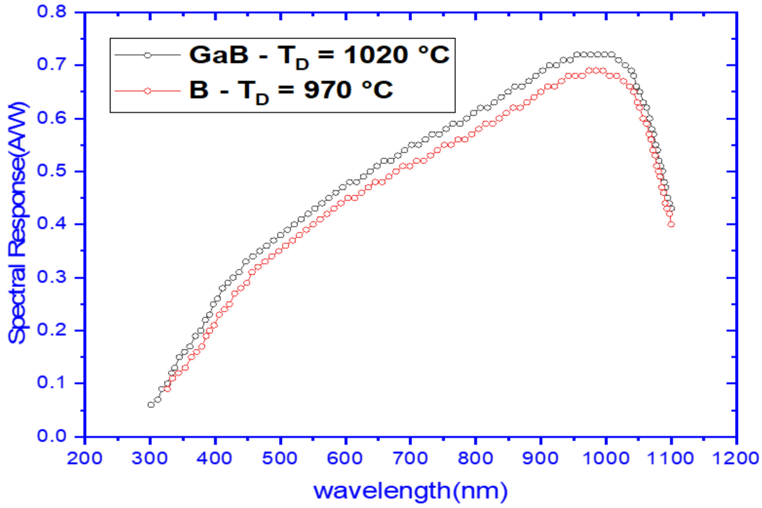


Figure 4. Spectral response of the best performing solar cells treated with B and GaB.

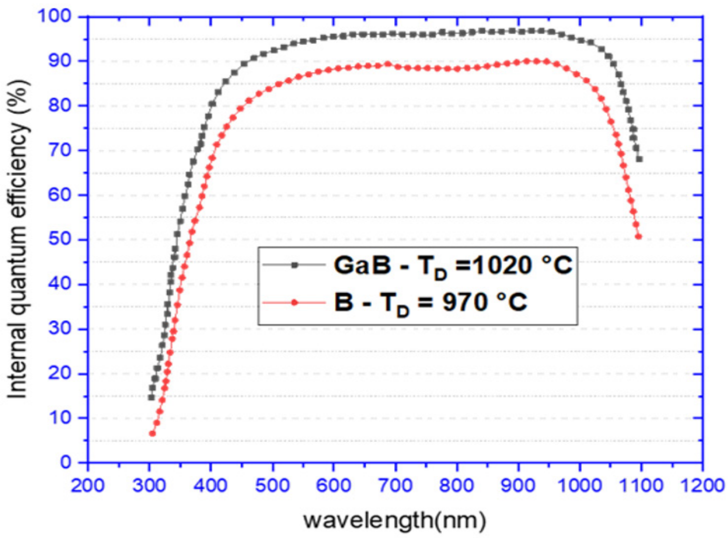


Figure 5. Internal quantum efficiency (%) (IQE) of the best performing solar cells treated with B and GaB.

## 4. CONCLUSIONS

This study evaluated the potential of aluminium, gallium and gallium/boron co-doping as p-type dopants in the production of thin n+np+ solar cells. The results clearly showed that aluminium is not suitable for the formation of the p+ emitter due to its low solubility and high segregation in silicon oxide. Gallium, on the other hand, required high diffusion temperatures and suffered from a degradation of the concentration profile in the later stages of the manufacturing process, leading to poor performing solar cells. Gallium/boron co-doping proved to be a promising alternative to boron, enabling thin n+np+ solar cells with a conversion efficiency of 13.7%. Although this performance is slightly lower than that of boron-doped cells (14.9%), it is encouraging and opens up interesting prospects for improving n+np+ cells. Optimisation of the GaB diffusion parameters, in particular temperature, time and atmosphere, as well as improved surface passivation, could reduce the parallel resistance observed in the cells and increase their efficiency.
The use of boron-gallium has several potential advantages over boron. The ability to diffuse GaB at lower temperatures could minimise thermal damage to thin substrates and improve the lifetime of charge carriers. In addition, the presence of gallium in the emitter could help to reduce the sensitivity of the cells to transition metals.
This study has highlighted the potential of gallium/boron co-doping for the manufacture of next-generation thin n+np+ solar cells. Further research is needed to optimise the manufacturing processes and fully exploit the benefits of this promising technology.

**Author Contributions:** Korichi: Developed the original idea and objectives and wrote the majority of the manuscript, including the introduction and discussion sections. Boucheham: Assisted in analyzing and interpreting the results, wrote sections, and participated in visualizing results in tables and figures. Kezrane: Discussed the implications and future perspectives, provided knowledge and expertise to enhance overall quality, reviewed the manuscript, suggested modifications, and assisted in the final preparation of the manuscript for submission.
**Data Availability Statement:** Not applicable.
**Funding:** The authors declare that no funds, grants, or other supports were received during the preparation of this manuscript.
**Conflicts of Interest:** The authors declare that they have no conflict of interest.
**Acknowledgments:** This work is realized in DDCS/CRTSE Division. The authors are gratefully acknowledging the financial support of the General Direction of Scientific Research and Technological Development of Algeria (DGRSDT/MESRS).

## NOMENCLATURE

The symbols and abbreviations used in this manuscript:

| Symbol | Definition | Unit |
|---|---|---|
| R□ | Sheet resistance | Ω/□ |
| Voc | Open-circuit voltage | mV |
| Jsc | Short-circuit current density | mA/cm² |
| FF | Fill factor | - |
| H | Conversion efficiency | % |
| B | Boron | - |
| Ga | Gallium | - |

| | | |
|---|---|---|
| Al | Aluminum | - |
| GaB | Gallium-Boron (co-doped) | - |
| AlGa | Aluminum-Gallium (co-doped) | - |
| T° | Temperature | °C |
| TD | Diffusion time | min |

## REFERENCES


*[1] A. Alatrash, et al., ''Assessing the Viability of Solar and Wind Energy Technologies in Semi-Arid and Arid Regions: A Case Study of Libya's Climatic Conditions." Applied Solar Energy, vol. 80. no. 1. pp. 149–170, 2024. https://doi.org/10.3103/S0003701X24600218.*

*[2] K. Bakouri, et al., ''Learning lessons from Murzuq-Libya meteorological station: Evaluation criteria and improvement recommendations." Solar Energy and Sustainable Development Journal, vol.12, no.1, pp. 30–48. 2023. https://doi.org/10.51646/jsesd.v12i1.149.*

*[3] H. Korichi, A. Boucheham, A. Bensdira, and M. Kazerane, ''Advancements in Passivation and Metallization Techniques for n-Type Monocrystalline Silicon Solar Cells." Solar Energy and Sustainable Development Journal, vol.13, no.2, pp. 151–173. 2024. https://doi.org/10.51646/jsesd.v13i2.185.*

*[4] M. A. Green, ''Silicon solar cells: Evolution, high-efficiency design and efficiency enhancements," Solar Energy, vol. 208, p. 118165, 2023, https://doi.org/10.1016/j.solener.2020.118165.*

*[5] A. S. Kagilik, A. M. Tawel, ''Performance Analysis of 14 MW Grid-Connected Photovoltaic System" Solar Energy And Sustainable Development Journal, 4(1), 11–21. https://doi.org/10.51646/jsesd.v4i1.78.*

*[6] R. Schuh, M. Holm et R. Brendel, ''Origin and impact of process-induced defects in n-type silicon », Physica Status Solidi (RRL)." Rapid Research Letters, vol. 8, no,1, p. 133–147, 2014, https://doi.org/10.1002/pssr.201308366.*

*[7] H. Cheng et al., ''Emitter formation with boron diffusion from PECVD deposited boron-doped silicon oxide for high-efficiency TOPCon solar cells," Solar Energy Materials and.Solar Cells, vol. 240, p. 111713, 2022, https://doi.org/10.1016/J.SOLMAT.2022.111713.*

*[8] Q. Wang, et al.,"Boron tube diffusion process parameters for high-efficiency n-TOPCon solar cells with selective boron emitters." Solar Energy Materials and Solar Cells, vol. 253, p. 112231, 2023, https://doi.org/10.1016/j.solmat.2023.112231.*

*[9] N. E. Grant et al., "Gallium-Doped Silicon for High-Efficiency Commercial Passivated Emitter and Rear Solar Cells," vol. 2000754, pp. 1–8, 2021, doi: 10.1002/solr.202000754.*

*[10] J. Hwang, P. Ho, J. Lewis, and R. Campbell, ''Grain boundary diffusion of aluminum in polycrystalline silicon films," J. Appl. Phys., vol. 51, no 3, p. 1576–1581, 2008, https://doi.org/110.1063/1.327811.*

*[11] ''Grain boundary diffusion of aluminum in polycrystalline silicon films for Journal of Applied Physics - IBM Research", [Enligne]. Disponible sur: https://research.ibm.com/publications/grain-boundary-diffusion-of-aluminum-in-polycrystalline-silicon-films.*

*[12] N. Grant, T. Trupke, J. Weber, and K. McIntosh, ''Gallium-doped silicon for high-efficiency commercial passivated emitter and rear solar cells," Progress in Photovoltaics Research and Applications, vol. 23, no 12, p. 1904–1914, 2015, https://doi.org/10.1002/solr.202000754.*

*[13] L. Shao, J. Liu, Q. Y. Chen, and W. K. Chu, ''Boron diffusion in silicon: The anomalies and control by point defect engineering," Materials Science and Engineering: R: Reports, vol. 42, no. 3-4,*

*2003, https://doi.org/10.1016/j.mser.2003.08.002.*

*[14] A. El Amrani, A. Boucheham, A. Guendouzi, B. Labdelli, C. Nasraoui, R. Si-Kaddour, ''Co-Diffusion Processing of p+/n/n+ Structure for n-Type Silicon Solar Cells Using Boron Doped Paper Sheets", Silicon, vol. 14, no. 1, p. 223–228, 2022, https://doi.org/10.1007/s12.*

*[15] A. Boucheham, A. Elamrani, H. Timlelt, C. Nasraoui et A. Saibi, « Investigation of p+ emitter formation for n-type silicon solar cells application », Materials Research Express, vol. 6, no. 12, p. 125905, 2019, https://doi.org/10.1088/2053-1591/ab5a0c.".*

*[16] P. Pal, V. Swarnalatha, A. V. N. Rao, A. K. Pandey, H. Tanaka and K. Sato, ''High speed silicon wet anisotropic etching for applications in bulk micromachining: A review," Micro and Nano Systems Letters, vol. 9, no 1, p. 15, 2021, https://doi.org/10.1186/s40486-021-".*

*[17] J. Kim, D. Inns, K. Fogel and D. Sadana, ''Surface texturing of single-crystalline silicon solar cells using low density SiO2 films as an anisotropic etch mask," Solar Energy Materials and Solar Cells, vol. 94, no 12, p. 2091–2093, 2010, https://doi.org/10.1016/j.solmat.2010.06.026".*

*[18] B. Labdelli et al., ''Influence of Wafer Thickness and Screen-Printing Mesh Counts on the Al-BSF in Crystalline Silicon Solar Cells," J. Nano- Electron. Phys., vol. 15, no 6, p. 1–5, 2023, https://doi.org/10.21272/jnep.15(6).06027.*

*[19] A. A. Fashina et al., "Surface texture and optical properties of crystalline silicon substrates," J. Renew. Sustain. Energy, vol. 7, no. 6, 2015, https://doi.org/10.1063/1.4937117.*

*[20] A. El Amrani, L. Boutaleb, A. Boucheham, Y. Belkacem, and C. Nasraoui, Investigation of pre-deposition temperature effect on n+-BSF properties in co-diffusion process," Mater. Res. Express, vol. 5, no. 1, 2018, https://doi.org/10.1088/2053-1591/aaa693.*

*[21] M. Rauer, C. Schmiga, M. Hermle, and S. W. Glunz, "Passivation of Screen-Printed Aluminium-Alloyed Emitters for Back Junction N-Type Silicon Solar Cells," 24th Eur. Photovolt. Sol. Energy Conf. 21-25 Sept. 2009, Hamburg, Ger. 1059, no. September, pp. 1059–1062, 2009.*

*[22] L. Zhao, C.L. Zhou, H.L. Li, H.W. Diao, W.J. Wang, ''Design optimization of bifacial HIT solar cells on p-type silicon substrates by simulation," Solar Energy Materials and Solar Cells, vol. 92, no. 6, 2008, https://doi.org/10.1016/j.solmat.2008.01.018.*

*[23] B.Swatowska, T. Stapiński, K. Drabczyk, & P. Panek, ''The role of antireflective coatings in silicon solar cells-The influence on their electrical parameters." Optica Applicata, vol. 41, no. 2, 487–492. 2011. https://doi.org/Optica Applicata XLI(2):487.*

*[24] J. Schube, Metallization of Silicon Solar Cells with Passivating Contacts. 2020. [Online]. Available: https://www.reiner-lemoine-stiftung.de/pdf/dissertationen/Dissertation-Joerg_Schube.pdf.*